

# ROBUST MULTIOBJECTIVE CONTROL OF A VARIABLE SPEED WIND TURBINE

B. Boukhezzar, H. Siguerdidjane

SUPELEC

3, rue Joliot Curie

F-91192 Gif-sur Yvette cedex FRANCE

Email : boubekur.boukhezzar, Houria.siguerdidjane@supelec.fr

Tel : +33 1 69 85 13 83, Fax : +33 1 69 85 13 89

**Abstract**—The purpose of this work<sup>1</sup> is to develop a robust controller for variable speed wind turbine based on Multi-objective synthesis in order to optimize the wind energy capture in partial load operation (below the rated power), while minimizing the transient loads in the turbine shafts. A linear model of the wind turbine is first derived from a nonlinear aeroelastic model. Control objectives that associate  $H_2$  and  $H_\infty$  are formulated in LMI form which is known to offer powerful tools to mixed criterion optimization. The aim of this work is to show that Multi-channel method provides an efficient way to handle a Multi-objective synthesis in variable speed wind turbine control. Simulation results show good performance of the proposed control law when applied to the aeroelastic model under a stochastic wind profile.

**Index Terms**—Wind turbine, variable speed, multiobjective control,  $H_2/H_\infty$  control, aeroelastic models

## I. INTRODUCTION

Advances in wind turbine technology [1] made necessary the design of more powerful control systems. This is in order to improve wind turbines behavior, namely to make them more profitable and more reliable.

The control objective depends on the region where the wind turbine (WT) operates.

Wind turbine operation can be divided into two regions (Fig. 1) :

- Below rated wind speed (partial load)  
where  $v_1 < v < v_2$ .
- Above rated wind speed (full load)  
where  $v_2 < v < v_3$ .

$v$  is the mean wind speed.

The wind turbine is stalled for  $v < v_1$  and  $v > v_3$ .

Control system design objectives for each region can be specified by [2] :

- Limitation and smoothing of electrical power in the above rated power area.
- Generation of maximum power in the below rated power area.
- Minimization of transient loads in all turbine components.

Many control strategies have been proposed in the literature, based on LTI models. Classical controllers have been extensively used, particularly the PI regulator [3], [4]. Optimal control of wind turbines has been also used in the  $LQ$  [5], [6], and  $LQG$  form [2], [7].

Robust control of wind energy conversion systems (WECS) has been introduced in [8] and also used in [9] - [10].

An  $H_\infty$  approach using weighting filters for inputs and outputs is presented in [11].

However, as mentioned in [2], the drawback of the methods quoted previously remains in the fact that the control objectives used to controller synthesis are not well formulated to take into account the stochastic and dynamic aspects of the wind turbine control.

In the case of variable speed wind turbine (VSWT), control below rated power must achieve two functions : optimal rotational speed tracking with fast wind speed variations rejection and avoiding significant undergoing efforts (torques and forces) for wind turbine structure.

In [11], those two objectives are treated identically by synthesizing a controller that minimize the  $H_\infty$  norm of the transfer matrix between exogenous inputs (wind speed  $v$  and torque disturbance  $T_d$ ) and the observed outputs (tracking error and control signal).

As known, the  $H_\infty$  controller minimizes the worse case of the ratio between the  $L_2$  norms of input and output signals. But in the control problem considered here, it is necessary to minimize the effect of fast wind speed variation over a long horizon while avoiding to the wind turbine significant efforts peak. It is then necessary to use different criteria for each objective.

In this paper, a multiobjective  $H_2/H_\infty$  control is used to build robust controllers for a horizontal axis variable speed wind turbine.

This paper is organized as follows. Section II presents first the wind turbine model, the optimal power tracking problem is then formulated. This section ends with the linearized model of the aeroelastic wind turbine one. The multiobjective  $H_2/H_\infty$  control approach is presented in Section III. This approach leads to a robust controller that takes into account different design specifications. The formulation of the  $H_2/H_\infty$  problem into LMI is then

<sup>1</sup> This work has been carried out within the project Énergie launched by Supélec.

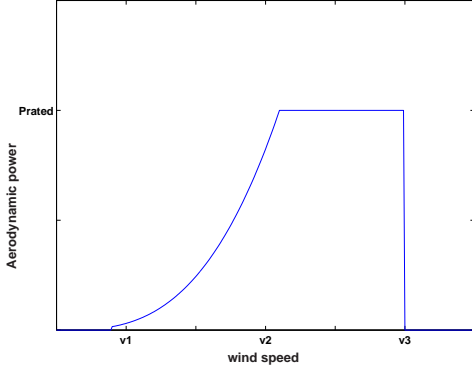


Fig. 1. Wind turbine power curve

exposed. In section IV, simulation results illustrate the performance of the proposed approach.

## II. WIND TURBINE MODELLING

### A. Model description

There are several classes of wind turbine simulators according to the objective of each one. Aeroelastic simulators are used to test loads supported by the wind turbine that is regarded as a flexible structure. The combined effects of aerodynamic loading of the wind, and the response of the turbine's structure, lead to complex simulators. Much efforts have been dedicated to the study of aeroelasticity, the main benefits that are expected from these simulations are the accurate prediction of loads and performance of a wind turbine rotor, a better understanding of the aeroelastic phenomenon, and finally the opportunity to test (and in a future perspective to tune) the semi-empirical engineering models. However, these models are too complex for controllers design, consequently engineering models must be obtained for control synthesis. Control models are simpler and easier to handle. They are generally represented by nonlinear or linear set of ordinary differential equations.

In this work, an aeroelastic simulator is used for open loop test, system linearization and synthesized control laws test. In engineering aeroelastic models, the aerodynamic loads are usually computed by semi-empirical models. However, these are relatively simplified models of the fluid flow dynamics, and therefore may lead to inaccurate results under certain conditions (particularly near and beyond stall, and for large amplitude deformations). At the same time, the increasing capabilities of modern computers have recently made possible the numerical simulation of fully three-dimensional viscous flows (also named as Computational Fluid Dynamics, or CFD) for some realistic engineering problems.

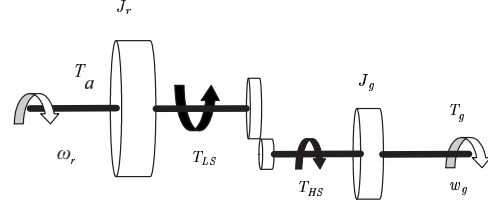


Fig. 2. Wind turbine scheme

### B. Problem formulation

The simplified wind turbine scheme is given in Fig. 2. The aerodynamic power captured from the wind is

$$P_a = \frac{1}{2} \rho \pi R^2 C_p(\lambda, \beta) v^3 \quad (1)$$

where

$$\lambda = \frac{\omega_r R}{v}$$

table of the symbols description is given at the end of this paper.

Using the relation

$$P_a = \omega_r T_a \quad (2)$$

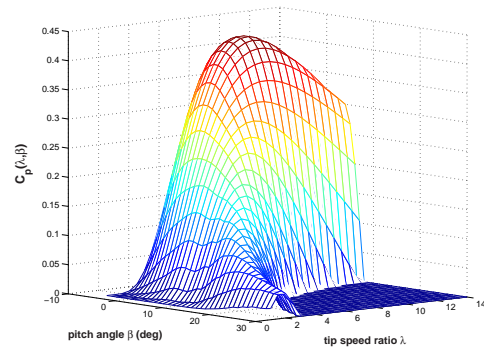
aerodynamic torque expression is

$$T_a = \frac{1}{2} \rho \pi R^3 C_q(\lambda, \beta) v^2 \quad (3)$$

with

$$C_q(\lambda, \beta) = \frac{C_p(\lambda, \beta)}{\lambda}$$

$C_p(\lambda, \beta)$  and  $C_q(\lambda, \beta)$  curves for the considered wind turbine are shown in Fig. 3 and Fig. 4.

Fig. 3.  $C_p(\lambda, \beta)$  curve

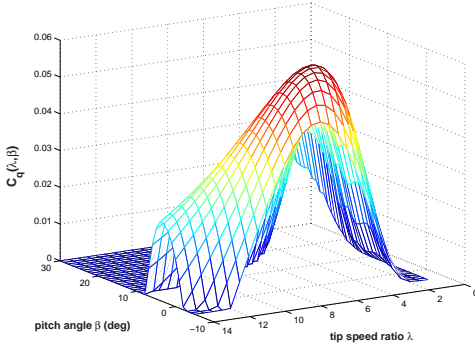


Fig. 4.  $C_p(\lambda, \beta)$  curve

The wind speed time repartition makes that, in most of time, the wind turbines are operating in wind speed less than rated one, hence the importance of control efficiency arises in this operating regime. While energy is captured from the wind, the aerodynamic power should be maximized below rated wind speed.

The  $C_p(\lambda, \beta)$  curve involved in the aerodynamic power expression (1) has a unique maximum (Fig. 3)

$$(\lambda, \beta) = (\lambda_{opt}, \beta_{opt}) \quad (4)$$

that corresponds to a maximum power production, where

$$\lambda_{opt} = \frac{\omega_r^* R}{v} \quad (5)$$

For this, in the below rated power area, to maximize wind power extraction, the blades pitch angle  $\beta$  is fixed to the optimal value  $\beta_{opt}$  and in order to make  $\lambda$  tracking its optimal value, the rotor speed must be adjusted to track the reference  $\omega_r^*$  which have the same shape as wind speed since they are proportional.

$$\omega_r^* = \frac{\lambda_{opt}}{R} v \quad (6)$$

the objective of the controller is to maximize wind power extraction by adjusting the rotor rotational speed  $\omega_r$  to wind speed variations such that the aerodynamic power stands at its maximum in spite of these variations.

### C. Linearized model

Linear state-space representation of the wind turbine is given by

$$\begin{cases} \dot{x} = Ax + Bu + B_d u_d \\ y = Cx + D_d u_d \end{cases} \quad (7)$$

the state vector  $x$  contains the deviation from the operating point of the activated degrees of freedom  $\Delta q$  of the simulator and their derivatives  $\Delta \dot{q}$ .

$$x = \begin{bmatrix} \Delta q \\ \Delta \dot{q} \end{bmatrix}$$

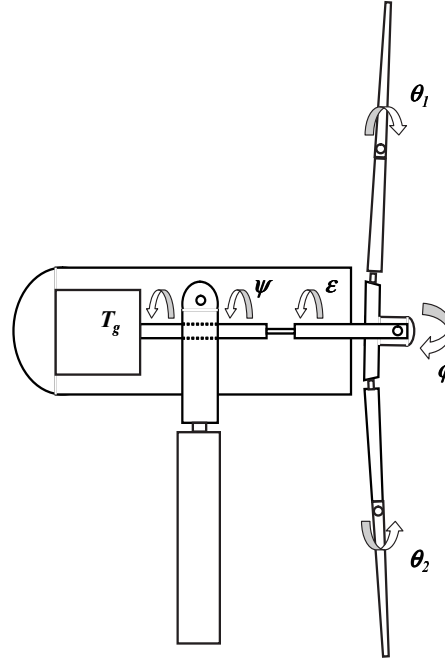


Fig. 5. Flexible Wind Turbine Degrees of Freedom

with

$$q = [\psi \ \varepsilon \ \varphi \ \theta_1 \ \theta_2]^T$$

$$\dot{q} = [\omega_r \ \dot{\varepsilon} \ \dot{\varphi} \ \dot{\theta}_1 \ \dot{\theta}_2]^T$$

The components of  $q$  shown in Fig. 5 are described in Fig. 6.

Symbol	Description
$\psi$	Generator Azimuth Position
$\varepsilon$	Shaft Torsional Deflection
$\varphi$	Hub Teeter
$\theta_1$	Blade #1 Flap angle
$\theta_2$	Blade #2 Flap angle

Fig. 6. Simulator Selected Degrees of Freedom

The linearized wind turbine model has two inputs : the wind speed  $v$  and the generator torque  $T_g$  that constitutes the control input.

$$\begin{bmatrix} u \\ u_d \end{bmatrix} = \begin{bmatrix} \Delta T_g \\ \Delta v \end{bmatrix} \quad (8)$$

The pitch angle of the blades is fixed to its optimal value. The choice of  $T_g$  as a control input is motivated by the fact that when connecting the generator to the grid via a frequency converter, the generator rotational speed  $\omega_g$  will be independent of the grid frequency. By controlling the firing angle of the converter, it is possible to control the electrical torque in the generator. The torque control using the frequency converter allows the wind turbine to run at

variable speed and thereby makes possible a reduction of the stress on the drive train and the gearbox [3]. The output  $y$  is the rotor speed tracking error

$$y = \Delta\omega_r - \frac{\lambda_{opt}}{R} \Delta v \quad (9)$$

### III. MUTIOBJECTIVE CONTROL

As already mentioned, the controller objectives are :

- 1) Minimizing the effect of wind speed fast variations
- 2) Reducing the stress undergoes by the wind turbine parts
- 3) Tracking the optimal rotor speed  $\omega_r^*$

The first objective can be achieved using an  $H_2$  criterion. It corresponds to the minimization of the wind speed disturbances effect over a long horizon. While the second is equivalent to avoid, to the wind turbine, significant effort peaks during wind speed peaks, thus the worst case. This can be reached using an  $H_\infty$  synthesis. In fact, the  $H_\infty$  norm minimize the worst case of the ratio between the  $H_2$  norm of the output  $T_{H_\infty}$  and the input  $x$

$$\|T_\infty(j\omega)\|_\infty = \sup_{\omega \in \mathbb{R}} \left[ \max_{x \in \mathbb{C}^n} \left[ \frac{\|T_\infty(j\omega)x\|_2}{\|x\|_2} \right] \right] \quad (10)$$

#### A. $H_2/H_\infty$ control

From the diagram of Fig. 7, the  $H_2$  (*resp.*  $H_\infty$ ) controller synthesis problem can be formulated as finding a controller  $K(s)$  over the set of all stabilizing controllers that minimizes the  $H_2$  (*resp.*  $H_\infty$ ) norm of the Linear Fractional Transformation (LFT)  $T_{zw}$

$$T_{zw} = G_{zu}(s)K(s)(I - G_{yu}(s)K(s))^{-1}G_{yw}(s) + G_{zw}$$

and where the  $H_2$  (*resp.*  $H_\infty$ ) norms of transfer matrix  $T$  are

$$\begin{aligned} \|T\|_2 &= \left( \frac{1}{2} \int_{-\infty}^{\infty} \text{trace}[T^*(j\omega)T(j\omega)] d\omega \right)^{1/2} \\ \|T\|_\infty &= \sup_{\omega} [\sigma_{max}(T(j\omega))] \end{aligned}$$

The problem solved in state space approach [12] gives a systematic approach for the synthesis of an optimal  $H_2$  or  $H_\infty$  controller using DGKF algorithm [13].

However, both standard approaches, used independently, are not adequate with all design specifications. For instance, noise attenuation or regulation against random disturbances are more naturally expressed in terms of  $LQG$ . Similarly, pure  $H_\infty$  synthesis only enforces closed-loop stability and does not allow of the closed-loop direct poles placement in more specific regions of the left-half plane [14].

The Multi-objective design procedures simultaneously take several performance criteria, the principle of these methods is to define several channels associated with different norms.

Mixed  $H_2/H_\infty$  is used in this work to reach design specifications described at the beginning of this section.

We then define two output channels associated with both

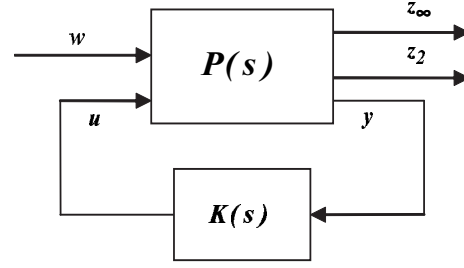


Fig. 7.  $H_2/H_\infty$  synthesis

$H_2$  and  $H_\infty$  criteria.

The output channel  $z_\infty$  is associated with the  $H_\infty$  performance while the channel  $z_2$  is associated with the  $LQG$  aspects ( $H_2$  performance in the case of white noise disturbance).

$$z = \begin{bmatrix} z_\infty \\ z_2 \end{bmatrix} = \begin{bmatrix} \Delta\varepsilon \\ \Delta\omega_r \end{bmatrix} \quad (11)$$

The problem became a multiobjective optimization problem consisting of minimizing the  $H_\infty$  of the  $T_\infty$  transfer under constraint on the  $H_2$  norm of the  $T_2$  transfer :

$$\min \|T_\infty\|_\infty \quad \text{under constraint} \quad \|T_2\|_2 < g \quad (12)$$

$T_2$  is the transfer matrix from  $w$  to  $z_2$  and  $T_\infty$  from  $w$  to  $z_\infty$ .

$$\begin{bmatrix} T_\infty \\ T_2 \end{bmatrix} = \begin{bmatrix} T_{z_\infty/w} \\ T_{z_2/w} \end{bmatrix} = \begin{bmatrix} T_{\Delta\varepsilon/\Delta v} \\ T_{\Delta\omega_r/\Delta v} \end{bmatrix}$$

#### B. LMI formulation

From the expression of  $z_\infty$ ,  $z_2$  and the state space equation (7), we can write

$$\begin{cases} \dot{x} &= Ax + B_1 w + B_2 u \\ z_\infty &= C_\infty x + D_{\infty 1} w + D_{\infty 2} u \\ z_2 &= C_2 x + D_{21} w + D_{22} u \\ y &= C_y x + D_{y1} w + D_{y2} u \end{cases} \quad (13)$$

such that

$$\begin{aligned} w &= \Delta v \quad ; \quad u = \Delta T_g \\ B_1 &= B_d \quad ; \quad B_2 = B \\ C_y &= C \quad ; \quad D_{y2} = D_d \end{aligned}$$

by setting

$$C_z = \begin{bmatrix} C_\infty \\ C_2 \end{bmatrix} \quad ; \quad D_{z1} = \begin{bmatrix} D_{\infty 1} \\ D_{21} \end{bmatrix}$$

$$D_{z2} = \begin{bmatrix} D_{\infty 2} \\ D_{22} \end{bmatrix}$$

it yields

$$\begin{bmatrix} \dot{x} \\ \vdots \\ z \\ y \end{bmatrix} = \begin{bmatrix} A & B_1 & B_2 \\ \vdots & \vdots & \vdots \\ C_z & D_{z1} & D_{z2} \\ C_y & D_{y1} & D_{y2} \end{bmatrix} \begin{bmatrix} x \\ w \\ u \end{bmatrix} \quad (14)$$

and finally in more compacted form

$$\begin{bmatrix} \dot{x} \\ \vdots \\ \mathcal{Y} \end{bmatrix} = \begin{bmatrix} \mathcal{A} & \mathcal{B} \\ \vdots & \vdots \\ \mathcal{C} & \mathcal{D} \end{bmatrix} \begin{bmatrix} x \\ w \\ \mathcal{U} \end{bmatrix} \quad (15)$$

with

$$\begin{aligned} \mathcal{A} &= A & ; & \quad \mathcal{B} = [B_1 \ B_2] \\ \mathcal{C} &= \begin{bmatrix} C_z \\ C_y \end{bmatrix} & ; & \quad \mathcal{D} = \begin{bmatrix} D_{z1} & D_{z2} \\ D_{y1} & D_{y2} \end{bmatrix} \end{aligned}$$

and

$$\mathcal{Y} = \begin{bmatrix} z \\ y \end{bmatrix} ; \quad \mathcal{U} = \begin{bmatrix} w \\ u \end{bmatrix}$$

$z$  defined in (11) is the performance channels vector. Its first component is the shaft torsional deflection  $\Delta\varepsilon$  associated with the  $H_\infty$  norm that is adapted to describe the stress undergone by the wind turbine. The second channel  $\Delta\omega_r$  is associated with the  $H_2$  norm more suitable to measure the reduction of wind turbulence effect on rotor speed along a large time interval. The controller  $K(s)$  computes the torque  $\Delta T_g$  from the output  $y = \Delta\omega_r - \frac{\lambda_{opt}}{R} \Delta v$  (Fig. 8).

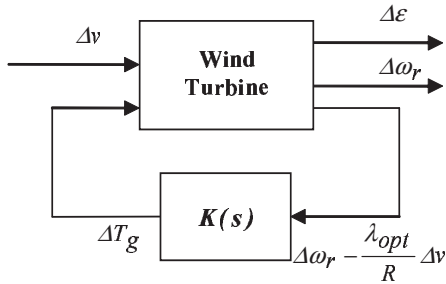


Fig. 8.  $H_2/H_\infty$  synthesis for the wind turbine

From the generalized state space representation (13), it is shown in [15], that one can construct, under certain conditions, a robust linear controller  $K(s)$  via LMI optimization of the multi-criterion problem (12).

The controller  $K(s)$  has the following state space representation

$$\begin{cases} \dot{\xi} &= A_K \xi + B_K u \\ y &= C_K \xi + D_K u \end{cases} \quad (16)$$

Details for controller synthesis are given in [15].

#### IV. SIMULATION RESULTS

The wind turbine considered in this study is a variable pitch, variable speed one. It consists of two blades rotor equipped with individual electromechanical pitch actuator. The rotor drives an induction generator.

The variable speed option interest comes out from the fact that it reduces stress due to the transient loads in the main shaft during the full load operation of the wind turbine and optimizes energy extraction over all wind speeds below rated. An additional benefit is that the variable speed turbines rotate not so much during their life time ; i.e. they can be brought to a lower rotational speed in the low wind speed region.

Open loop response for a wind speed profile is first tested on the aeroelastic simulator<sup>2</sup> before applying the proposed controllers. Both of rotor speed  $\omega_r$  and low speed shaft loads are obtained for a wind speed profile of 15 m/s mean value (Fig. 9).

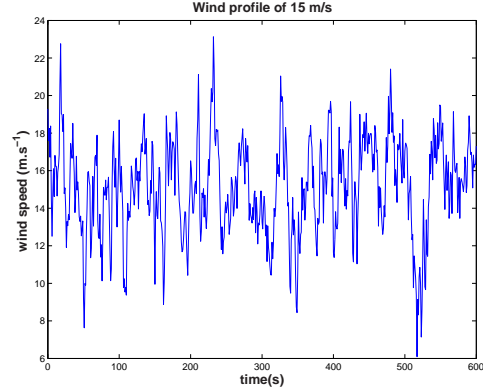
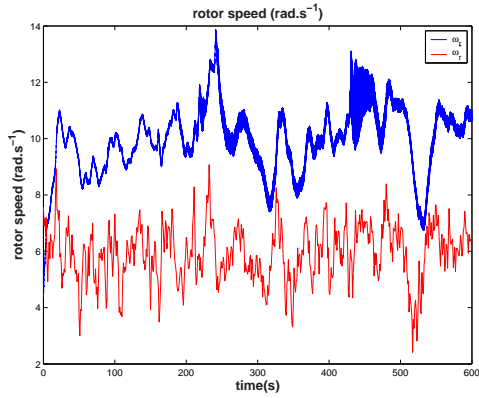


Fig. 9. Wind Speed Profile of 15  $m.s^{-1}$

As shown in Fig. 10(a), the open loop rotor speed  $\omega_r$  is compared to the optimal rotor speed  $\omega_r^*$  that ensure optimal power extraction from the wind. One can observe a significant error between  $\omega_r$  and  $\omega_r^*$ , this led to a poor aerodynamic efficiency and a large proportion of the energy contained in the wind is not captured. We can also notice from Fig 12(a) large oscillations in the rotor shaft torsional moment. We note a large variation and significant loads submitted to the rotor shaft.

<sup>2</sup>developed by NREL, Golden, CO.



(a) Open Loop

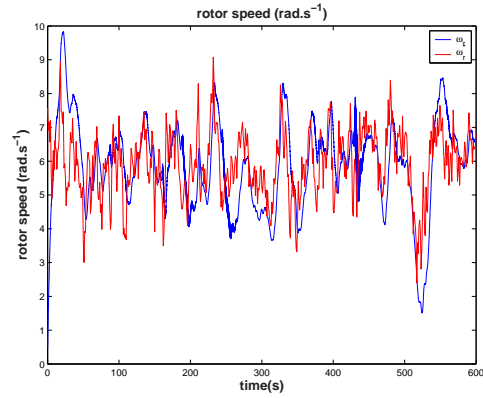
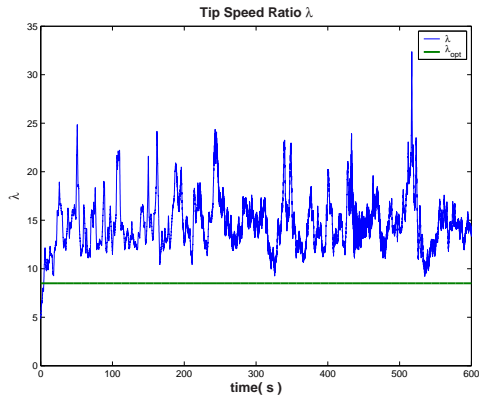
(b) Closed Loop with the  $H_2/H_\infty$  controller

Fig. 10. Optimal Rotor Speed Tracking



(a) Open Loop

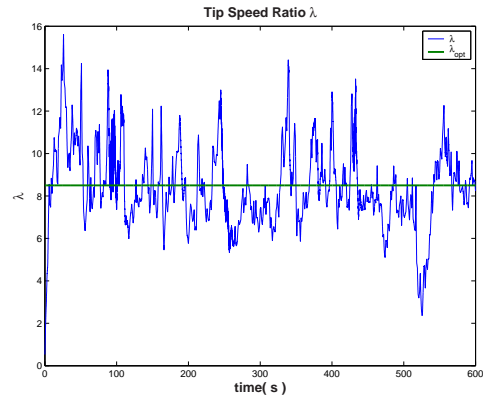
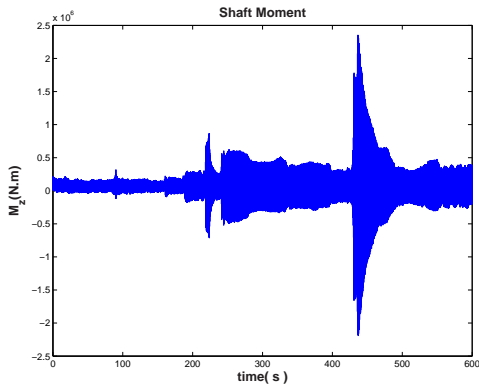
(b) Closed Loop with the  $H_2/H_\infty$  controller

Fig. 11. Tip Speed Ratio



(a) Open Loop

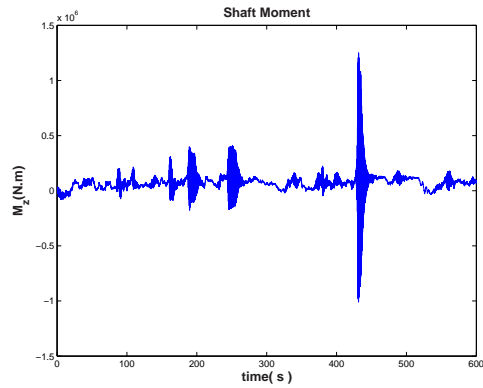
(b) Closed Loop with the  $H_2/H_\infty$  controller

Fig. 12. Shaft Torsional Moment

In order to improve wind power capture and reduce the mechanical loads, the proposed multiobjective  $H_2/H_\infty$  controllers schemes have been applied to the aeroelastic model under the same wind profile. The  $H_2/H_\infty$  controller synthesis is based on the linearized model described in the subsection II-C. The linearized state-space representation of the wind turbine is first obtained, then the constrained optimization problem (12) is formulated into LMI constraints. The obtained controller  $K(s)$  is thus tested on the aeroelastic simulator for the same wind profile (Fig. 9). The rotor speed  $\omega_r$  with the  $H_2/H_\infty$  controller  $K(s)$  is compared to the optimal rotor speed  $\omega_r^*$  defined in (6). Results are shown in Fig. 10(b). One may observe that the controller achieves a good optimal rotor speed tracking performance in spite of wind speed turbulence. This increases the wind power capture, indeed, as one can see in Fig. 11(b), the tip speed ratio  $\lambda$  remains close to the optimal value  $\lambda_{opt}$  with the  $H_2/H_\infty$  controller compared to the open loop (Fig. 11(a)). As mentioned in Fig. 13, the aerodynamic efficiency of wind turbine with the  $H_2/H_\infty$  controller is better than the open loop one. Generally, good tracking performance lead to significant loads in the wind turbine parts. The minimization of the  $H_\infty$  norm of the transfer matrix  $\|T_{\Delta\varepsilon/\Delta v}\|_\infty$  between the wind speed  $v$  and the shaft torsional deflexion  $\varepsilon$  under constraint on the upper limit to the  $H_2$  norm, have permitted to reduce and limit rotor shaft loads while optimizing the capture of the wind energy. The shaft torsional moment with the  $H_2/H_\infty$  controller is shown in Fig. 12(b). The aerodynamic efficiency, the Shaft Torsional Moment standard deviation and peak value are given in Fig. 13 for the open and closed loop.

	Open Loop	$H_2/H_\infty$ Controller
Aerodynamic efficiency	51.44 %	92.64 %
Torsional Torque Standard Deviation [N.m]	$3.21 \cdot 10^5$	$2.35 \cdot 10^5$
Torsional Torque peak value [N.m]	$2.35 \cdot 10^6$	$1.25 \cdot 10^6$

Fig. 13. Aerodynamic efficiency and Torsional Torque

We can note a low moment loads in spite of the good tracking performance with the  $H_2/H_\infty$  controller. The Shaft Torsional Moment in Closed Loop peak value is reduced by 80 % compared with the Open Loop while the aerodynamic efficiency is widely greater than Closed Loop. This is achieved by the controller synthesis criterion that is a compromise between the reduction of the turbulence effect on rotor speed and loads on the rotor shaft.

## V. CONCLUSION

This work emphasizes the performance of multiobjective  $H_2/H_\infty$  control technics for optimal power curve tracking

problem of a wind turbine. This multi-criterion has led to the synthesis of robust controller satisfying two objectives : Tracking optimal power curve and reducing shaft loads. This could not be formulated with the same performance criterion (or norm).

In addition, it has been also shown a good level of robustness, by using these controllers, in comparison with the as well as satisfactory results in presence of high level turbulence in the wind speed.

## NOTATION AND SYMBOLS

$v$	wind speed ( $\text{m} \cdot \text{s}^{-1}$ ).
$\rho$	air density ( $\text{kg} \cdot \text{m}^{-3}$ ).
$R$	rotor radius (m).
$P_a$	aerodynamic power (W).
$T_a$	aerodynamic torque ( $\text{N} \cdot \text{m}$ ).
$\lambda$	tip speed ratio.
$C_p(\lambda)$	power coefficient.
$C_q(\lambda)$	torque coefficient.
$\omega_r$	rotor speed ( $\text{rad} \cdot \text{s}^{-1}$ ).
$\omega_r^*$	rotor speed reference ( $\text{rad} \cdot \text{s}^{-1}$ ).
$T_g$	generator (electromagnetic) torque ( $\text{N} \cdot \text{m}$ ).
$T_{LS}$	low speed shaft ( $\text{N} \cdot \text{m}$ ).
$T_{HS}$	high speed shaft ( $\text{N} \cdot \text{m}$ ).
$J_r$	rotor inertia ( $\text{kg} \cdot \text{m}^2$ ).
$J_g$	generator inertia ( $\text{kg} \cdot \text{m}^2$ ).
$\varepsilon$	shaft torsional deflexion (deg).
$\psi$	generator azimuth position (deg).
$\varphi$	hub teeter (deg).

## ACKNOWLEDGMENT

The authors would like to thank M. Hand and E. Muljadi from NREL for their great help in providing the simulator, thus giving us the opportunity to validate our theoretical results.

## REFERENCES

- [1] L. V. Divone, *Evolution of modern wind turbines*, ch. 3, pp. 73–138. David A. Sepra, amse press ed., 1995.
- [2] W. E. Leithead, S. DeLaSalle, and D. Reardon, "Role and objectives of control of wind turbines," *IEEE Proceedings Part C*, vol. 138, pp. 135–148, 1991.
- [3] X. Ma, *Adaptive extremum control and wind turbine control*. PhD thesis, Technical University of Denmark, 1997.
- [4] M. M. Hand and M. J. Balas, "Non-linear and linear model based controller design for variable-speed wind turbines," pp. 1–8. NREL Report No. CP-500-26244.
- [5] E. S. Abdin and W. Xu, "Control design and dynamic performance analysis of a wind turbine-induction generator unit," *IEEE Transactions on energy conversion*, vol. 15, no. 1, pp. 91–96, 2000.
- [6] T. Ekelund, *Modeling and Linear Quadratic Optimal Control of Wind Turbines*. PhD thesis, Chalmers University of Technology, Sweden, April 1997.
- [7] P. Novak, T. Ekelund, I. Jovilk, and B. Schmidtbauer, "Modeling and control of variable speed wind turbine drive systems dynamics," *IEEE Control Systems Magazine*, vol. 15, no. 4, pp. 28–38, 1995.



- [8] M. Steinbuch, *Dynamic modelling and robust control of a wind energy conversion system*. PhD thesis, Delft University of Technology, Netherlands, 1989.
- [9] P. Bongers, *Modeling and identification of flexible wind turbines and a factorizational approach to robust control*. PhD thesis, Delft University of Technology, Netherlands, 1994.
- [10] D. Connor, S. N. Iyer, W. E. Leithead, and M. J. Grimble, "Control of horizontal axis wind turbine using  $h_\infty$  control," *First IEEE Conference on Control Applications*, 1992.
- [11] R. Rocha, P. Ressende, J. L. Silvino, and M. Bortolus, "Control of stall regulated wind turbine through  $h_\infty$  loop shapping method," *IEEE International Conference on Control Applications*, 2001.
- [12] J. C. Doyle, K. Glover, P. P. Khargonekar, and B. A. Francis, "State-space solution to standard  $h_2$  and  $h_\infty$  control problem," *IEEE Transactions on automatic control*, vol. 34, no. 8, pp. 831–847, 1989.
- [13] K. Zhou, J. C. Doyle, and K. Glover, *Robust and Optimal Control*. Prentice Hall, 1995.
- [14] P. Gahinet, A. Nemirovski, A. J. Laub, and M. Chilali, *LMI Control Toolbox*. Paris : The Mathworks, Inc., 1995.
- [15] C. Scherer, P. Gahinet, and M. Chilali, "Multiobjective output-feedback control via lmi optimization," *IEEE Transactions on automatic control*, vol. 42, no. 7, pp. 896–911, 1997.